HHS Public Access

Author manuscript

Exp Gerontol. Author manuscript; available in PMC 2016 March 01.

Published in final edited form as:

Exp Gerontol. 2015 March ; 63: 48–58. doi:10.1016/j.exger.2015.01.048.

Effect of *in vivo* loading on bone composition varies with animal age

Marta Aido[a,b], **Michael Kerschnitzki**[c,b], **Rebecca Hoerth**[c,b], **Sara Checa**[a], **Lyudmila Spevak**[e], **Adele Boskey**[e], **Peter Fratzl**[c,b], **Georg N. Duda**[a,b,d], **Wolfgang Wagermaier**[c], and **Bettina M. Willie**[a,*]

[a]Julius Wolff Institute, Charité-Universitätsmedizin Berlin, Germany

[b]Berlin Brandenburg School for Regenerative Therapies (BSRT), Berlin, Germany

[c]Max Planck Institute of Colloids and Interfaces, Potsdam, Germany

[d]Berlin Brandenburg Center for Regenerative Therapies (BCRT), Berlin, Germany

[e]Hospital for Special Surgery, New York, NY, USA

Abstract

Loading can increase bone mass and size and this response is reduced with aging. It is unclear, however how loading affects bone mineral and matrix properties. Fourier Transform Infrared Imaging and high resolution synchrotron scanning small angle X-ray scattering were used to study how bone's microscale and nanoscale compositional properties were altered in the tibial midshaft of young, adult, and elderly female C57Bl/6J mice after two weeks of controlled *in vivo* compressive loading in comparison to physiological loading. The effect of controlled loading on bone composition varied with animal age, since it predominantly influenced the bone composition of elderly mice. Interestingly, controlled loading led to enhanced collagen maturity in elderly mice. In addition, although the rate of bone formation was increased by controlled loading based on histomorphometry, the newly formed tissue had similar material quality to new bone tissue formed during physiological loading. Similar to previous studies, our data showed that bone

*Corresponding author: Willie, B.M., Julius Wolff Institute, Charité - Universitätsmedizin Berlin, Augustenburger Platz 1, 13353 Berlin, Germany, Tel: +49 (0)30 450 559589, Fax: +49 (0)30 450 559938, bettina.willie@charite.de.

Each author's postal addresses:

Aido, M., Julius Wolff Institute, Charité - Universitätsmedizin Berlin, Augustenburger Platz 1, 13353 Berlin, Germany.
Kerschnitzki, M., Max Planck Institute of Colloids and Interfaces, Am Mühlenberg 1, 14476 Potsdam, Germany.
Hoerth, R., Max Planck Institute of Colloids and Interfaces, Am Mühlenberg 1, 14476 Potsdam, Germany.
Checa, S., Julius Wolff Institut, Charité - Universitätsmedizin Berlin, Augustenburger Platz 1, 13353 Berlin, Germany.
Spevak, L., Research Department, Hospital for Special Surgery, 535 E 70th Street, New York, NY 10021
Boskey, A., Research Department, Hospital for Special Surgery, 535 E 70th Street, New York, NY 10021
Fratzl,P., Max Planck Institute of Colloids and Interfaces, Am Mühlenberg 1, 14476 Potsdam, Germany.
Duda, G.N., Julius Wolff Institut, Charité - Universitätsmedizin Berlin, Augustenburger Platz 1, 13353 Berlin, Germany.
Wagermaier, W., Max Planck Institute of Colloids and Interfaces, Am Mühlenberg 1, 14476 Potsdam, Germany.

Conflict of Interest

All authors state that they have no conflicts of interest.

composition was animal and tissue age dependent during physiological loading. The findings that the new tissue formed in response to controlled loading and physiological loading had similar bone composition and that controlled loading enhanced bone composition in elderly mice further supports the use of physical activity as a noninvasive treatment to enhance bone quality as well as maintain bone mass in individuals suffering from age-related bone loss.

Keywords

Bone adaptation; Tibial Compression; Aging; Bone quality; synchrotron sSAXS; FTIRI

1. Introduction

Bone has the ability to adapt to its mechanical environment, attaining an optimized structure that fulfills its mechanical and homeostatic functions. However, bone fragility is known to increase with aging, leading to an increased risk of fracture. Age-related changes in bone mass have been extensively studied. However, changes in bone mass alone do not explain the increased fragility and fracture risk of elderly individuals [1, 2]. It has become apparent that the quality of bone tissue, which includes the microscale and nanoscale properties of its mineral particles and organic matrix also contributes to the increased fragility of bone with aging [3].

Physical activity is thought to be a promising noninvasive treatment for people suffering from age-related bone loss. Interestingly, human exercise [4–9] and preclinical studies [10–12] indicate that the adaptive bone formation response to mechanical loading diminishes with age. While it is known that moderate strain levels induce increases in bone mass and bone size and this effect is reduced with aging, less is known on how loading affects bone compositional properties [13, 14]. Loading may alter bone quality by affecting the basic constituents of bone tissue: mineral and/or collagen. Human exercise studies have shown inconsistent effects on volumetric bone density [15] with several preclinical studies demonstrating that mechanical loading had no effect on bone density [16–19], while others have shown increases in bone density [20–23]. It has also been suggested that loading alters the orientation of the extrafibrillar mineral [24–26]. In all of these studies, mechanical loading induced bone formation, but the authors did not differentiate between tissue quality changes in newly formed and pre-existing tissue. However, one study by Kohn et al. [27] used a short-term exercise regime (21 days) in 16 week old C57Bl/6 male mice that did not increase bone formation, assessed by histomorphometry. They showed loading increased structural and tissue level mechanical properties by altering bone quality of pre-existing tissue via enhanced mineralization (increased mineral:matrix ratio), mineral composition (decreased carbonate:phosphate ratio) and the organic matrix (increased collagen maturity).

It has been reported that exercise-induced changes in bone composition are inbred mouse strain [28] and gender [29] specific; aging may also influence the adaption of bone composition to mechanical loading. Most studies examining if bone composition is influenced by loading have focused on young animals or examined how exercise early in life may have long-lasting effects later in life [19, 30]. Unfortunately, few studies have

examined the effect of loading on bone composition in older animals. Isaksson et al. [31] showed in decalcified humeri from C57Bl/6 male mice, that voluntary exercise (continuous access to a running wheel beginning at age 1 month old) led to improved tensional properties of the collagen network when the mice were still young and growing (2 and 4 month old), but not when the mice were adults (6 month old). The authors attributed the exercise-related improved mechanical properties in the young mice to increased remodeling of the bone, along with reorientation of the collagen fibrils. Additionally, they measured no difference between running mice compared to sedentary controls of any age in the collagen content or crosslinks measured via high-performance liquid chromatography. Interestingly, a subsequent study [32] reported that 17 months of voluntary exercise in 18 month old C57Bl/6 male mice had no effect on the amount of collagen or its crosslinks, reduced tensile properties of the bone collagen, reduced diaphyseal cortical BMD, but increased diaphyseal cortical bone stiffness in running mice compared to sedentary controls. Unfortunately the authors could not directly compare how age (2, 4, 6 and 18 month old mice) influenced the effect of exercise on bone composition, since the duration of exercise for each group was different (1, 3, 5, and 17 months of voluntary exercise, respectively).

Previous studies analyzing how bone composition is influenced by loading used models such as voluntary exercise that may have included varied levels of physical activity between animals and did not allow for controlled loading conditions, such as strain or load-matched comparisons between age groups. In earlier studies [33, 34], we found that two weeks of strain-matched (1200 microstrain engendered at the tibial midshaft) controlled *in vivo* loading led to increased bone formation in 10, 26 and 78 week old female C57Bl/6J mice although the bone formation response was reduced with maturation and aging [10, 12]. While changes in bone's mass and architecture with loading were confirmed, it is unclear whether changed loading conditions altered the mineral and matrix properties. We were particularly interested in learning if the increased mineral apposition rate occurring in response to controlled loading altered bone composition, since our co-authors [35] previously reported that bone tissue rapidly formed via intramembranous ossification during healing has altered mineral and matrix properties. Therefore, we used Fourier Transform Infrared Imaging (FTIRI) and high resolution (1μm) synchrotron scanning small-angle X-ray scattering (sSAXS) to assess the molecular composition and nanoscale physical properties of bone's mineral and matrix, which have been shown to be important determinants of bone tissue quality [3, 36–39]. Our first aim was to examine the effects of mechanical loading on bone's quality and in particular to analyze the mineral and matrix properties of new tissue, formed in response to *in vivo* loading (compared to physiological loading). Our second aim was to study how bone's mineral and matrix properties are dependent on both animal age (adolescent, adult and elderly mice) and tissue age (intracortical, endosteal and periosteal regions) during physiological loading.

2. Materials and Methods

2.1 In vivo mechanical loading

Twenty-one female C57Bl/6J mice (n=7/age: young 10 week old, adult 26 week old, and elderly 78 week old) purchased from Jackson Laboratory (Sulzfeld, Germany) were housed

3 to 5 per cage with *ad libitum* access to food and water. All animal experiments were carried out according to the policies and procedures approved by the local legal research animal welfare representative (LAGeSo Berlin, G0333/09). All mice underwent *in vivo* cyclic compressive loading of the left tibia. The mouse's knee and ankle were positioned in the loading device into concave cups, through which a 1 N preload was applied (Testbench ElectroForce LM1, Bose, Framingham, USA) (Figure 1A). Loading parameters included: 216 cycles applied daily at 4 Hz, 5 days/week (M-F), for 2 weeks, delivering -9N (78 week old mice) or -11N (10 and 26 week old mice) peak loads. Previous *in vivo* strain gauging studies demonstrated that these peak load values were required to engender a strain of approximately 1200 με at the tibial midshaft [33, 34]. The triangle waveform applied included 0.15 sec symmetric active loading/unloading, 0.1 sec rest insertion (at 1N) between load cycles and a 5 sec pause between every four cycles. The right tibia served as an internal control. Calcein was administered via intraperitoneal injection at a dose of 30 μg/g, 12 and 3 days before euthanasia. Mice were sacrificed on day 15, three days after the last loading session, while under anesthesia through an overdose of potassium chloride. After *in vivo* loading, both the left and right tibiae of the animals were dissected from the surrounding soft tissues. All tibiae were embedded in polymethyl methacrylate (PMMA) (Technovit 9100, Wehreim, Germany). Tibiae from fifteen mice (n=5 mice/age) were analyzed with FTIRI and tibiae from six mice (n=2/age) were studied with sSAXS.

2.2 Dynamic Histomorphometry

Endosteal and periosteal bone formation indices of both control and *in vivo* loaded tibiae of 10, 26 and 78 week old mice (n=5/age) were determined. The 10 and 26 week old mice were a subset from a larger group, which was previously reported [33]. Sections were imaged and analysed with a fluorescent microscope (Leica DMRB, Munich, Germany and AxioCam MRc, Zeiss, Oberkochen, Germany) at a magnification of 200×. The entire endocortical (Ec) and periosteal (Ps) surfaces were measured. Outcome parameters, the single- and double-labeled surface per bone surface (sLS/BS, dLS/BS), mineralizing surface (MS/BS), mineral apposition rate (MAR), and bone formation rate (BFR/BS), were analyzed as recommended by the American Society for Bone and Mineral Research [40].

2.3 Sample preparation for FTIRI and sSAXS

The control and the *in vivo* loaded tibiae from fifteen mice (n=5 mice/age) were cut in the transverse plane at the midshaft with a microtome (Leica SM2500S, Munich, Germany) into 2.5 μm thick sections for FTIRI imaging. The control and the *in vivo* loaded tibiae from six mice (n=2 mice/age) were microtomed into 10 μm thick sections in a direction parallel to the longitudinal axis of the long bones for synchrotron sSAXS measurements. All sections were imaged with fluorescence microscopy (Leica DMRB, Munich, Germany), before being measured with FTIRI or sSAXS.

2.4 FTIRI data acquisition and analysis

The prepared undecalcified tibial sections were mounted on barium fluoride infrared windows for FTIRI (Perkin Elmer Spotlight Imaging System). Three regions of cortical bone, periosteal, endosteal, and intracortical, at the posterior side of the midshaft of the

control and the *in vivo* loaded tibiae were analyzed using a spectral resolution of 4 cm^{-1} and a spatial resolution of 6.25 μm. The posterior side was chosen based on finite element models indicating higher compressive strains in this region [41]. Based on the histomorphometry data and the resolution of the FTIRI technique, periosteal and endosteal regions were defined as having a width of approximately 20 μm starting from the bone surface. The intracortical region included all the bone tissue within a 50 μm region, centered within the middle of the bone. The following FTIRI parameters were calculated (ISYS software) based on the spectrum of bone (Figure 1D): mineral:matrix ratio (area of 916–1180 cm^{-1}/1590–1712 cm^{-1}), which relates with the amount of mineral present, carbonate:mineral ratio (area of 852–890 cm^{-1}/916–1180 cm^{-1}), which reflects the level of carbonate substitution in the mineral particles, collagen maturity (peak intensity ratio of 1660 cm^{-1}/1690 cm^{-1}), crystallinity (peak intensity ratio of 1020 cm^{-1}/1030 cm^{-1}), which relates with the size and perfection of the mineral particles [42] and acid phosphate content (peak height 1096 cm^{-1}/1128 cm^{-1}), the level of acid phosphate substitution in the mineral particles.

2.5 sSAXS data acquisition

The midshaft region of the control and the *in vivo* loaded tibiae (125–300 μm × 30–77.5 μm) was examined by sSAXS at the nanofocus beamline (ID 13) at the European Synchrotron Radiation Facility (ESRF) in Grenoble, France. Three regions of interest were studied within the midshaft: periosteal, endosteal, and intracortical regions. To include only newly formed tissue based on the calcein labeling and due to the high resolution of the sSAXS method, we defined the periosteal and endosteal regions as regions with a width of approximately 10 μm starting from the bone surface. The intracortical region included all the bone tissue (approximately 150 μm wide) starting 40 μm away from each bone surface, to assure a separation from the endosteal and periosteal regions. Although the sSAXS measurements were performed in mice of all three age groups, only data from the 10 week old mice was used to compare newly tissue formed from additional *in vivo* loading to that formed from physiological loading in the control limbs. This was due to the limited to sometimes negligible amounts of newly formed tissue in the two adult and two elderly mice, while the young mice still had rapidly forming new bone in the endosteal and periosteal regions of the control limbs, identified by calcein labeling. Sample scan locations were defined through the use of a long-distance optical microscope. A monochromatic high energy (15 keV) X-ray beam with a wavelength of 0.0812 nm and a diameter of 1 μm was used to scan the samples, with a step size of 1 μm within the plane perpendicular to the incident beam. The sSAXS patterns were captured with an ESRF FreLoN detector (up to more than 20,000 SAXS diffraction patterns collected per sample), placed at 539 mm from the sample and the exposure time was set between 0.6 and 0.8 seconds. The detector had an active area of 2048 × 2048 pixels and a pixel size of 51.7 μm × 51.5 μm. To speed up data acquisition, a detector binning of 4 × 4 was used, which corresponded to a pixel size of 206.9 μm × 206.2 μm. A silver behenate standard was used for an accurate calibration of the X-ray beam center and the sample to detector distance.

2.6 sSAXS data correction and analysis

All the 2D sSAXS patterns were corrected for dark current (CCD readout noise) and rescaled for beam intensity fluctuations from ESRF source and absorption effects in the samples. The patterns were radially and azimuthally integrated to a function I(q) and I(χ), respectively, where I is the scattering intensity, q the scattering length (relates to the scattering angle θ by the equation ($q=(4\pi/\lambda)\sin(\theta/2)$) and χ the azimuthal angle. These calculations were performed with Autofit (C. Li, Max Planck Institute of Colloids and Interfaces, Potsdam, Germany). From the resulting function I(q) and based on Porod's law, the T parameter, the average mineral particle thickness in the scattering volume, was calculated. T is defined as $T=(4\Phi(1-\Phi))/\sigma$, where Φ is the volume of mineral per tissue volume and σ the surface area of mineral per tissue volume [43]. For thin platelet shaped mineral particles and if mineral volume fraction is in the range of 0.5, T is a measure of the particle smallest dimension corresponding to the mean mineral thickness (Figure 1B). The function I(χ) was used to derive the degree of alignment of the mineral particles within the plane perpendicular to the primary beam, the ρ parameter [43]. The ρ parameter is defined as $\rho=A_1/(A_1+A_0)$, where A_0 is the total sSAXS intensity caused by randomly oriented particles and A_1 the sSAXS intensity due to particles aligned parallel to a certain direction. For a perfect alignment of mineral particles, ρ=1 and the sSAXS pattern is a narrow line perpendicular to the long axis of the particles, while for randomly oriented mineral particles, ρ=0 and the sSAXS pattern is circular (Figure 1C).

2.7 Statistical analysis

For FTIRI, the within-subject effect of loading (loaded, control limbs) and region of interest (endosteal, intracortical, periosteal) and the between-subject effects of age (10, 26, 78 week old) and interactions were assessed using a repeated measures ANOVA (SAS 9.3, Cary, NC, USA). For FTIRI, paired t-tests were performed to determine the effect of loading (loaded, control limbs) or the effect of region of interest (endosteal, intracortical, periosteal) within each age group. Unpaired t-tests were performed to determine the effect of animal age (10, 26 and 78 week old mice) within *in vivo* loaded and control tibiae. All values are presented as mean ± standard deviation and statistical significance was set at $p<0.05$. All reported results are significant unless otherwise stated. Only descriptive statistics are given for the data obtained with sSAXS measurements, due to the limited sample size.

3. Results

3. 1 Effect of in vivo loading on bone composition is animal age-dependent

3.1.1 Young mice—Loading led to a significant increase in nearly all the measured histomorphometric indices (Ec.MAR, Ec.BFR/BS, Ps.dLS/BS, Ps.MS/BS, Ps.MAR, Ps.BFR/BS) (Table 2), but we measured no difference in any of the measured FTIRI parameters between loaded and control limbs at the endosteal or periosteal regions of 10 week old mice (Figure 3). We detected a significantly greater acid phosphate content at the intracortical region of the loaded limbs, when compared to the control limbs (Table 1, Figure 2). The sSAXS measurements at the endosteal and periosteal regions (newly formed tissue, identified by fluorochrome labeling) were only performed in the loaded and control limbs of the two 10 week old mice (Figure 3) as they were still rapidly forming bone in both

the loaded and control limbs, evidenced by the histomorphometric analysis. Within the intracortical region of the loaded limb, there was a +1.9 % and a +2 % change in the T parameter, relative to the control limb for the two 10 week old mice (Figure 4A and B).

3.1.2 Adult mice—In the 26 week old mice, loading only affected the periosteal region, where the mineral crystallinity and acid phosphate were significantly greater in the loaded limbs than the control limbs. However, loading led to significantly greater Ec. MAR and Ec. BFR/BS (marginally significant) compared to control limbs (Table 2). Within the intracortical region, the mean T parameter changed −2.5 % and −3.5 %, relative to the control limb of each of the two 26 week old mice (Figure 4A and B).

3.1.3 Elderly mice—In the 78 week old mice, there was a significantly greater collagen maturity at the intracortical region of the loaded limbs compared to the control limbs (Table 1, Figure 2). The average mineral:matrix ratio was 12 % higher in the loaded limbs than in the control limbs of elderly mice, but this difference was not significant (Table 1). Additionally, we measured a significantly greater collagen maturity in the periosteal region of loaded compared to control limbs (Table 1, Figure 2). The mineral:matrix ratio in the endosteal region was also significantly greater in the loaded compared to the control limbs. None of the histomorphometric indices were significantly affected by loading (Table 2). The sSAXS analysis showed that the average T parameter in the loaded limb changed −6.4 % and +7.8 %, relative to the control limb of each of the two studied 78 week old mice (Figure 4A and B).

3.2 Animal age significantly affected bone's mineral and matrix properties

All five parameters studied with FTIRI were significantly altered by animal age (Table 1). In the intracortical region, between 10 and 26 week old mice, there was no significant increase in the mineral:matrix ratio ($p= 0.07$ for control limbs, $p=0.09$ for loaded limbs) and a significant increase of carbonate:mineral ratio for both loaded and control limbs. However, there was a decrease of crystallinity in the control limbs of 26 week old, when compared to 10 week old mice. Between 26 and 78 week old mice, there was an increase in the loaded limbs in collagen maturity and in both limbs in crystallinity and a decrease in carbonate:mineral ratio (in the loaded limb) and acid phosphate (in both limbs). The T parameter at the intracortical region varied between 2.3 and 2.4, between 2.3 and 2.6 and between 2.2 and 2.7 in the 10, 26 and 78 week old mice, respectively (loaded and control limbs). Therefore, the highest value of mean T parameter (T=2.7 nm) was registered in the control limbs of one of the 78 week old animals (Figure 4A). The ρ parameter varied between 0.47 and 0.62, between 0.45 and 0.56 and between 0.53 and 0.59 at the intracortical region of 10, 26 and 78 week old mice, respectively (Figure 4B). In the endosteal and periosteal region, between 10 and 26 and between 26 and 78 week old mice, no significant differences were detected in any of the measured parameters in the control limbs. In the loaded limbs there was an increase in carbonate:mineral ratio in the periosteal region between 10 and 26 week old mice, while between 26 and 78 week old mice, there was an increase in collagen maturity and a decrease in acid phosphate in both regions. There was also an increase in mineral:matrix ratio in the endosteal region, between 26 and 78 week old mice. All the endocortical histomorphometric indices, except Ec.MAR significantly

increased with age. At the periosteal region, only Ps.MS/BS was significantly changed with age (Table 2).

3.3 Tissue age significantly affected bone's mineral and matrix properties

Tissue age based on the region of interest (young bone in the periosteal and endosteal regions, mature bone in the intracortical region) significantly influenced all the parameters analyzed with FTIRI (Table 1). The endosteal and periosteal regions of both the loaded and control limbs of the 10, 26 and 78 week old mice had lower mineral:matrix ratio (Figure 5) and crystallinity (with few, marginally significant exceptions: p=0.07 for loaded limbs of 26 week old and p=0.06 for control limbs of 78 week old, for periosteal versus intracortical region comparisons) and higher acid phosphate than the intracortical region. The endosteal and periosteal regions of the control limbs of 10 week old mice had significant or close to significant (p=0.06, periosteal versus intracortical region) lower collagen maturity than the intracortical region. In addition, carbonate:mineral ratio was lower in the periosteal region than in the intracortical region of both limbs of the 10 week old mice and the loaded limbs of the 26 week old mice. Carbonate:mineral ratio was higher in the periosteal region of the control limbs of the 78 week old mice, than in the intracortical region (Table 1).

3.4 Mineral and matrix properties of new tissue formed in response to controlled loading differed regionally

Significant differences were noted in the mineral and matrix properties of the newly formed tissue at the endosteal region compared to the periosteal region of the tibiae of 10 week old mice. A significantly lower mineral:matrix ratio and significantly greater carbonate:mineral ratio was measured at the endosteal compared to the periosteal region of the loaded tibiae (Table 1). When comparing the new tissue formed in response to controlled loading, the sSAXS measurements showed that there was a +24.0 % and a +12.2 % change in the average T parameter in the periosteal compared to the endosteal region for each of the two 10 week old mice studied. The average ρ parameter in the periosteal region changed +8.6 % and +17.3 % relative to the endosteal region for each of the two mice studied (Figure 6).

4. Discussion

We and others [10, 11] have shown that the bone formation response to mechanical loading diminishes with increasing age and that there is already a dramatic reduction in mechanoresponsiveness at skeletal maturation in female C57Bl/6J mice. Less is known about the influence of mechanical loading on the tissue material properties of both the pre-existing and newly formed bone. Thus, the present study examined the bone's micro and nanoscale mineral and matrix properties in young, adult and elderly female C57Bl/6J mice after two weeks of controlled noninvasive *in vivo* tibial compressive loading and physiological loading. We use C57Bl/6J mice as a model for age-related bone loss, since this strain undergoes more cortical and trabecular bone loss with aging than other mouse strains [44–47] and similar to humans [48], cancellous bone loss begins in adulthood in C57Bl/6J mice. Additionally, previous loading and unloading studies [49, 50], have shown increased mechanoresponsiveness in C57Bl/6J mice compared to other mouse strains. Interestingly, our data indicated that the effect of *in vivo* loading on bone composition varied

with animal age, since controlled loading-induced changes in bone composition were predominantly observed in elderly mice. Controlled *in vivo* loading led to enhanced collagen maturity (at the periosteal and intracortical regions) and mineral:matrix ratio (at the endosteal region) in elderly mice. It has been suggested that the degree of bone mineralization depends on the maturation of the collagen network [51, 52]. In contrast to our findings in elderly mice, bone composition was largely unaltered by loading in young mice, as only significantly greater acid phosphate content (at the intracortical region) was measured. Similarly in adult mice, only mineral crystallinity and acid phosphate content (both at the periosteal region) were enhanced by controlled loading. In contrast to our results where we saw controlled loading enhanced collagen maturity in elderly, but not in young or adult C57Bl/6 female mice, Isaksson et al [31, 32] reported that voluntary exercise (continuous access to a running wheel beginning at age 1 month old) led to improved tensional properties of the collagen network in young (2 and 4 month old) mice, but not in adult (6 month old) or elderly (18 month old) C57Bl/6 male mice, compared to sedentary controls. However, they measured no difference in the collagen content or crosslinks between running mice compared to sedentary controls of any age. It is difficult to compare our study to theirs since we used strain-matched controlled loading over 15 days, whereas the previous studies included 1–17 months of voluntary exercise, which likely engendered different strain levels in the tibia during physical activity for the different aged mice. Unfortunately, besides the above mentioned investigations, no others studies have examined the effect of altered loading conditions on bone composition in elderly animals.

The effect of *in vivo* loading on bone composition did not seem to vary with tissue age, although there were some region-specific (endosteal, periosteal, and intracortical region which reflects tissue age) differences between loaded and control limbs observed in elderly mice. Additionally, when comparing new tissue formed in the loaded limbs with new tissue formed in the control limbs of the 10 week old mice; the age group that had the largest amount of new tissue formed during the experiment period, no change in mineral and matrix properties was detected. These findings suggest that two weeks of *in vivo* loading increased the rate of bone formation as confirmed by MAR, but the newly formed bone in response to *in vivo* loading does not have altered mineral and matrix properties, when compared to bone formed during physiological loading. These data indicate that tissue formed during controlled loading does not compromise bone quality, which in exercised adult humans might influence the patient’s risk of fracture. This is an important finding since mechanical loading has been seen as a promising treatment strategy to combat age-related bone loss. It was previously unclear whether the increased mineralization rate, due to the mechanical loading regime, altered the bone quality since earlier studies have shown that bone tissue rapidly formed via intramembranous ossification during healing has altered mineral and matrix properties [35, 53]. To our knowledge there are no previous studies that have compared how altered loading conditions affect the bone composition of newly formed tissue.

In agreement with earlier data [54–56], animal age had a significant effect on the mineral and matrix properties measured with FTIRI. With the intracortical region, we could detect a significant difference between young (10 week old) and adult (26 week old) mice and

between adult and elderly (78 week old) mice. A significant increase in carbonate:mineral ratio and a 14.2 % (p=0.07) and 12.7 % (p=0.09), respective increase in mineral:matrix ratio was observed for both control and loaded limbs between 10 and 26 week old, but not between 26 and 78 week old mice. This result supports the idea that mineral:matrix and carbonate:mineral ratios increase markedly only up to adulthood. Similar findings were reported for both FTIRI parameters in a study examining bone composition in baboon femora [54]. The decrease detected in acid phosphate content in both limbs between 26 and 78 week old mice relates to the finding that acid phosphate substitution in the mineral lattice reflects new mineral deposition [57]. Acid phosphate content is a more recently validated FTIRI parameter, however a decrease in acid phosphate content was observed in mice up to 6 months old [57]. No changes were detected in collagen maturity with animal aging in the control limbs, similar to previous reports [58–61]. Crystallinity, which reflects both the mineral size and perfection, varied in absolute values only slightly between the studied animal ages (between 1.11 and 1.19 in control limbs and between 1.12 and 1.20 in loaded limbs). Although the highest mean T parameter was detected in the control limb of an elderly mouse, the mean values for this parameter were similar between the studied ages. This finding is supported by studies that showed that the mean T parameter increases only up to 2 to 3 months in mice femora and tibiae (8 months was the maximum age studied) [62] and that it remains substantially the same throughout life in human femora [63]. Additionally, a study of vertebrae from 15 week old up to 97 years old individuals, showed a rapid increase in mineral thickness up to the age of four years old, followed by only subtle increases in thickness after this age [64]. The ρ parameter at the intracortical region of the loaded and control limbs had similar values for all the studied ages: 10, 26 and 78 week old mice. This result is consistent with studies that reported no change in the ρ parameter with increasing age in mice [62] and in the degree of preferred mineral orientation after the first decade of life in human femora [63].

The tissue in the endosteal and periosteal regions did not differ significantly between 10 and 26 or between 26 and 78 week old mice in the control limbs. For the loaded limbs, almost no difference was detected between 10 and 26 week old mice, while there were some differences measured between 26 and 78 week old mice. The differences encountered in the loaded limbs could be related to greater tissue age differences in the endosteal and periosteal regions between 26 and 78 week old mice, as there is a greater amount of newly formed tissue in the loaded limbs of 26 week old mice, in comparison with control limbs. In general, these results indicate that mineral and matrix properties of tissue in the endosteal and periosteal regions are similar, independent of the age of the animal.

Since the effects of animal age and tissue age on bone’s mineral and matrix properties are often intermixed in the literature, we evaluated the effects of each, separately. As with animal age, tissue age was shown to have a significant effect on the mineral and matrix properties studied with FTIRI. Similar to previous studies, we detected lower mineral:matrix ratio [54, 56, 59, 65, 66] and crystallinity [54, 65, 66] and higher acid phosphate content [57, 67, 68] in the younger tissue at the periosteal and endosteal regions, when compared with older intracortical tissue within mice of all three ages studied. The increased acid phosphate content in these regions corresponds to the previously reported acid phosphate substitution in areas of new bone formation [57, 67, 68]. Collagen maturity, which has been shown to

increase with tissue age [42, 54, 66], was only lower in the endosteal and periosteal region when compared to intracortical region, in the control limbs of 10 week old mice, the age with the highest amount of newly formed tissue. The parameter carbonate:mineral ratio has been reported both to increase [42, 54, 56], and to decrease [69, 70] with tissue aging. In our study, we saw that the tissue at the periosteal side of the bone had lower carbonate:mineral ratio than the intracortical mature tissue in young and adult animals, but higher carbonate:mineral ratio in elderly mice. We have seen that the mean mineral thickness and degree of alignment tended to be lower in the newly formed tissue at the endosteal region, but not at the periosteal region, when compared to older tissue in the intracortical region. The variation of T and ρ parameters with tissue age was previously shown, as smaller T and ρ parameters were detected in the young tissue close to the center of osteons in human femora, when compared to tissue further away from the center [71]. In addition, smaller ρ parameters were measured in tissue close to the trabeculae surface (compared with older tissue in the middle of the trabeculae) [72] and smaller T parameters were detected in younger tissue adjacent to the endosteal surface in rat femora (compared to intracortical tissue) [73].

Interestingly, the newly formed tissue at the periosteal region of the bone was composed of mineral particles with a higher degree of alignment and greater thickness than the newly formed tissue at the endosteal region. The new tissue at the periosteal region also had a greater mineral:matrix and carbonate:mineral ratio than the tissue at the endosteal region. These data suggest that the periosteal region is more mineralized and thus the endosteal region was younger bone, which is reflected in the greater mineral apposition rate at the endosteal compared to the periosteal region. The periosteal region is thought to experience higher strain levels than the endosteal region during controlled loading, which may explain the higher degree of alignment of the mineral particles at this region. A previous study by Akkus et al. [69] also reported greater mineralization at the periosteal compared to the endosteal region, measured using Raman microspectroscopy in middle-aged rat femora.

Our study is not without limitations. Conclusions based on the sSAXS data are limited by the sample size of 6 tibiae (n=2 mice/age). These measurements were performed during a 96 hour session at the ESRF, a facility where usage is very restricted. However, we were able to measure each sample with extremely high resolution, collecting up to more than 20,000 single scattering patterns per sample, measured with 1 μm spacing between each other. Choosing a small beam size (1 μm) allowed a robust measurement of mineral properties within small regions of newly formed tissue at the endosteal and periosteal regions. However, this meant that the spatial resolution of the sSAXS and FTIRI measurements were different. In addition, the calculation of the T parameter was based on the assumption that mineral volume fraction was approximately 0.5. The mineral:matrix ratio obtained in our study indicates that volume mineral fraction might not strongly deviate from 0.5. Although it would have been possible to obtain information on the real width W of the plate-like mineral particles, this would have required combining sSAXS with quantitative backscattered electron imaging (qBEI) measurements to determine the volume fraction of the mineral particles; this analysis would have gone beyond the scope of the current study. The calculation of the W parameter has been described previously [74]. Another limitation of our study was that the endosteal and periosteal regions analyzed with FTIRI did not always

strictly correspond to bone tissue located between calcein labels. Nevertheless, the chosen endosteal and periosteal region of interest (approximately 20 μm) included younger tissue with significantly lower mineral:matrix ratio, crystallinity and higher acid phosphate content than the intracortical mature tissue region. The differences between loaded limbs and control limbs were generally much smaller than the differences between endosteal or periosteal and the intracortical region for each mouse, reinforcing our finding that *in vivo* loading did not affect the quality of the newly formed tissue. In addition, even though we separately analyzed the influence of animal age and tissue age on bone's mineral and matrix properties, one shouldn't forget that the differences detected between young and older mice are not necessarily linked to a real animal aging effect. Young mice may be different from older mice because, due to fast growth, even their "old" bone is comparatively younger than "old" bone in older mice.

5. Conclusion

The effect of controlled loading on bone composition varied with animal age, since loading-induced adaptive changes in the mineral and matrix properties were predominantly observed in elderly mice. Interestingly, controlled loading led to enhanced collagen maturity in the elderly mice. In addition, although the rate of bone formation was increased by controlled loading based on histomorphometry, the newly formed tissue had similar material quality to new bone tissue formed during physiological loading. Although further studies with longer loading durations are required, the current findings suggest that mechanical loading is a promising noninvasive treatment to enhance bone quality as well as maintain bone mass in individuals suffering from age-related bone loss.

Acknowledgments

This study was supported by the German Federal Ministry of Education and Research (BMBF; Osteopath/TP6), the German Research Foundation (DFG; WI 3761/1-1, WI 3761/4-1, DU 298/14-1, CH 1123/4-1), the European Synchrotron Radiation Facility (SC-3308) and the National Institutes of Health (NIH grants AR041325 and AR046121).

References

1. Schuit SC, van der Klift M, Weel AE, de Laet CE, Burger H, Seeman E, Hofman A, Uitterlinden AG, van Leeuwen JP, Pols HA. Fracture incidence and association with bone mineral density in elderly men and women: the Rotterdam Study. Bone. 2004; 34(1):195–202. [PubMed: 14751578]
2. Marshall D, Johnell O, Wedel H. Meta-analysis of how well measures of bone mineral density predict occurrence of osteoporotic fractures. BMJ. 1996; 312(7041):1254–1259. [PubMed: 8634613]
3. Gourion-Arsiquaud S, Faibish D, Myers E, Spevak L, Compston J, Hodsman A, Shane E, Recker RR, Boskey ER, Boskey AL. Use of FTIR spectroscopic imaging to identify parameters associated with fragility fracture. J Bone Miner Res. 2009; 24(9):1565–1571. [PubMed: 19419303]
4. Fuchs RK, Bauer JJ, Snow CM. Jumping improves hip and lumbar spine bone mass in prepubescent children: a randomized controlled trial. J Bone Miner Res. 2001; 16(1):148–156. [PubMed: 11149479]
5. Kerr D, Morton A, Dick I, Prince R. Exercise effects on bone mass in postmenopausal women are site-specific and load-dependent. J Bone Miner Res. 1996; 11(2):218–225. [PubMed: 8822346]

6. Kohrt WM, Ehsani AA, Birge SJ Jr. Effects of exercise involving predominantly either joint-reaction or ground-reaction forces on bone mineral density in older women. J Bone Miner Res. 1997; 12(8):1253–1261. [PubMed: 9258756]
7. Bassey EJ, Rothwell MC, Littlewood JJ, Pye DW. Pre- and postmenopausal women have different bone mineral density responses to the same high-impact exercise. J Bone Miner Res. 1998; 13(12): 1805–1813. [PubMed: 9844097]
8. Kontulainen S, Sievanen H, Kannus P, Pasanen M, Vuori I. Effect of long-term impact-loading on mass, size, and estimated strength of humerus and radius of female racquetsports players: a peripheral quantitative computed tomography study between young and old starters and controls. J Bone Miner Res. 2003; 18(2):352–359. [PubMed: 12568413]
9. Kato T, Terashima T, Yamashita T, Hatanaka Y, Honda A, Umemura Y. Effect of low-repetition jump training on bone mineral density in young women. J Appl Physiol (1985). 2006; 100(3):839–843. [PubMed: 16269526]
10. Birkhold AI, Razi H, Duda GN, Weinkamer R, Checa S, Willie BM. Mineralizing surface is the main target of mechanical stimulation independent of age: 3D dynamic in vivo morphometry. Bone. 2014; 66:15–25. [PubMed: 24882735]
11. Holguin N, Brodt MD, Sanchez ME, Silva MJ. Aging diminishes lamellar and woven bone formation induced by tibial compression in adult C57BL/6. Bone. 2014; 65:83–91. [PubMed: 24836737]
12. Birkhold AI, Razi H, Duda GN, Weinkamer R, Checa S, Willie BM. The influence of age on adaptive bone formation and bone resorption. Biomaterials. 2014 In press.
13. Forwood MR, Burr DB. Physical activity and bone mass: exercises in futility? Bone and mineral. 1993; 21(2):89–112. [PubMed: 8358253]
14. Pearson OM, Lieberman DE. The aging of Wolff's "law": ontogeny and responses to mechanical loading in cortical bone. American journal of physical anthropology. 2004; (Suppl 39):63–99. [PubMed: 15605390]
15. Polidoulis I, Beyene J, Cheung AM. The effect of exercise on pQCT parameters of bone structure and strength in postmenopausal women--a systematic review and meta-analysis of randomized controlled trials. Osteoporosis international : a journal established as result of cooperation between the European Foundation for Osteoporosis and the National Osteoporosis Foundation of the USA. 2012; 23(1):39–51.
16. Umemura Y, Ishiko T, Yamauchi T, Kurono M, Mashiko S. Five jumps per day increase bone mass and breaking force in rats. J Bone Miner Res. 1997; 12(9):1480–1485. [PubMed: 9286765]
17. Jarvinen TL, Pajamaki I, Sievanen H, Vuohelainen T, Tuukkanen J, Jarvinen M, Kannus P. Femoral neck response to exercise and subsequent deconditioning in young and adult rats. J Bone Miner Res. 2003; 18(7):1292–1299. [PubMed: 12854840]
18. Woo SL, Kuei SC, Amiel D, Gomez MA, Hayes WC, White FC, Akeson WH. The effect of prolonged physical training on the properties of long bone: a study of Wolff's Law. The Journal of bone and joint surgery American volume. 1981; 63(5):780–787. [PubMed: 7240300]
19. Firth EC, Rogers CW, van Weeren PR, Barneveld A, McIlwraith CW, Kawcak CE, Goodship AE, Smith RK. Mild exercise early in life produces changes in bone size and strength but not density in proximal phalangeal, third metacarpal and third carpal bones of foals. Veterinary journal. 2011; 190(3):383–389.
20. Chow JW, Jagger CJ, Chambers TJ. Characterization of osteogenic response to mechanical stimulation in cancellous bone of rat caudal vertebrae. The American journal of physiology. 1993; 265(2 Pt 1):E340–E347. [PubMed: 8368304]
21. Darby LA, Pohlman RL, Lechner AJ. Increased bone calcium following endurance exercise in the mature female rat. Laboratory animal science. 1985; 35(4):382–386. [PubMed: 4046548]
22. Kesavan C, Mohan S, Oberholtzer S, Wergedal JE, Baylink DJ. Mechanical loading-induced gene expression and BMD changes are different in two inbred mouse strains. Journal of applied physiology. 2005; 99(5):1951–1957. [PubMed: 16024522]
23. Tidswell HK, Innes JF, Avery NC, Clegg PD, Barr AR, Vaughan-Thomas A, Wakley G, Tarlton JF. High-intensity exercise induces structural, compositional and metabolic changes in cuboidal bones--findings from an equine athlete model. Bone. 2008; 43(4):724–733. [PubMed: 18619567]

24. Takano Y, Turner CH, Owan I, Martin RB, Lau ST, Forwood MR, Burr DB. Elastic anisotropy and collagen orientation of osteonal bone are dependent on the mechanical strain distribution. Journal of orthopaedic research : official publication of the Orthopaedic Research Society. 1999; 17(1):59–66. [PubMed: 10073648]
25. Skedros JG, Sorenson SM, Takano Y, Turner CH. Dissociation of mineral and collagen orientations may differentially adapt compact bone for regional loading environments: results from acoustic velocity measurements in deer calcanei. Bone. 2006; 39(1):143–151. [PubMed: 16459155]
26. Turner CH, Chandran A, Pidaparti RM. The anisotropy of osteonal bone and its ultrastructural implications. Bone. 1995; 17(1):85–89. [PubMed: 7577163]
27. Kohn DH, Sahar ND, Wallace JM, Golcuk K, Morris MD. Exercise alters mineral and matrix composition in the absence of adding new bone. Cells Tissues Organs. 2009; 189(1–4):33–37. [PubMed: 18703871]
28. Wallace JM, Golcuk K, Morris MD, Kohn DH. Inbred strain-specific effects of exercise in wild type and biglycan deficient mice. Annals of biomedical engineering. 2010; 38(4):1607–1617. [PubMed: 20033775]
29. Wallace JM, Rajachar RM, Allen MR, Bloomfield SA, Robey PG, Young MF, Kohn DH. Exercise-induced changes in the cortical bone of growing mice are bone- and gender-specific. Bone. 2007; 40(4):1120–1127. [PubMed: 17240210]
30. Koistinen AP, Halmesmaki EP, Iivarinen JT, Arokoski JP, Brama PA, Jurvelin JS, Helminen HJ, Isaksson H. Short-term exercise-induced improvements in bone properties are for the most part not maintained during aging in hamsters. Experimental gerontology. 2014; 51:46–53. [PubMed: 24423444]
31. Isaksson H, Tolvanen V, Finnila MA, Iivarinen J, Tuukkanen J, Seppanen K, Arokoski JP, Brama PA, Jurvelin JS, Helminen HJ. Physical exercise improves properties of bone and its collagen network in growing and maturing mice. Calcif Tissue Int. 2009; 85(3):247–256. [PubMed: 19641838]
32. Isaksson H, Tolvanen V, Finnila MA, Iivarinen J, Turunen A, Silvast TS, Tuukkanen J, Seppanen K, Arokoski JP, Brama PA, Jurvelin JS, Helminen HJ. Long-term voluntary exercise of male mice induces more beneficial effects on cancellous and cortical bone than on the collagenous matrix. Exp Gerontol. 2009; 44(11):708–717. [PubMed: 19706321]
33. Willie BM, Birkhold A, Razi H, Thiele T, Aido M, et al. Diminished response to in vivo mechanical loading in trabecular and not cortical bone in adulthood of female C57Bl/6 mice coincides with a reduction in deformation to load. Bone. 2013; 55(2):335–346. [PubMed: 23643681]
34. Pflanz, D.; Berthet, E., et al. No Additive Effects of In Vivo Loading and Sclerostin Antibody Treatment on Bone Anabolism in Elderly Mice; ASBMR 2012 Annual Meeting; 2012.
35. Liu Y, Manjubala I, Schell H, Epari DR, Roschger P, Duda GN, Fratzl P. Size and habit of mineral particles in bone and mineralized callus during bone healing in sheep. J Bone Miner Res. 2010; 25(9):2029–2038. [PubMed: 20225262]
36. Fratzl P, Gupta HS, Paschalis EP, Roschger P. Structure and mechanical quality of the collagen–mineral nano-composite in bone. Journal of Materials Chemistry. 2004; 14(14):2115–2123.
37. Wang X, Shen X, Li X, Agrawal CM. Age-related changes in the collagen network and toughness of bone. Bone. 2002; 31(1):1–7. [PubMed: 12110404]
38. Kerschnitzki M, Kollmannsberger P, Burghammer M, Duda GN, Weinkamer R, Wagermaier W, Fratzl P. Architecture of the osteocyte network correlates with bone material quality. J Bone Miner Res. 2013; 28(8):1837–1845. [PubMed: 23494896]
39. Bar-On B, Wagner HD. The emergence of an unusual stiffness profile in hierarchical biological tissues. Acta Biomater. 2013; 9(9):8099–8109. [PubMed: 23669625]
40. Dempster DW, Compston JE, Drezner MK, Glorieux FH, Kanis JA, Malluche H, Meunier PJ, Ott SM, Recker RR, Parfitt AM. Standardized nomenclature, symbols, and units for bone histomorphometry: a 2012 update of the report of the ASBMR Histomorphometry Nomenclature Committee. J Bone Miner Res. 2013; 28(1):2–17. [PubMed: 23197339]

41. Razi H, Birkhold A, Zaslansky P, Weinkamer R, Duda G, Willie B, Checa S. Aging leads to a reduction in the load transmission within the bone: a murine tibia study. Bone. 2014 under review.
42. Boskey A, Pleshko Camacho N. FT-IR imaging of native and tissue-engineered bone and cartilage. Biomaterials. 2007; 28(15):2465–2478. [PubMed: 17175021]
43. Rinnerthaler S, Roschger P, Jakob HF, Nader A, Klaushofer K, Fratzl P. Scanning small angle X-ray scattering analysis of human bone sections. Calcif Tissue Int. 1999; 64(5):422–429. [PubMed: 10203419]
44. Jilka RL. The relevance of mouse models for investigating age-related bone loss in humans. J Gerontol A Biol Sci Med Sci. 2013; 68(10):1209–1217. [PubMed: 23689830]
45. Halloran BP, Ferguson VL, Simske SJ, Burghardt A, Venton LL, Majumdar S. Changes in bone structure and mass with advancing age in the male C57BL/6J mouse. J Bone Miner Res. 2002; 17(6):1044–1050. [PubMed: 12054159]
46. Glatt V, Canalis E, Stadmeyer L, Bouxsein ML. Age-related changes in trabecular architecture differ in female and male C57BL/6J mice. J Bone Miner Res. 2007; 22(8):1197–1207. [PubMed: 17488199]
47. Brodt MD, Silva MJ. Aged mice have enhanced endocortical response and normal periosteal response compared with young-adult mice following 1 week of axial tibial compression. J Bone Miner Res. 2010; 25(9):2006–2015. [PubMed: 20499381]
48. Khosla S. Pathogenesis of age-related bone loss in humans. J Gerontol A Biol Sci Med Sci. 2013; 68(10):1226–1235. [PubMed: 22923429]
49. Akhter MP, Cullen DM, Pedersen EA, Kimmel DB, Recker RR. Bone response to in vivo mechanical loading in two breeds of mice. Calcif Tissue Int. 1998; 63(5):442–449. [PubMed: 9799831]
50. Amblard D, Lafage-Proust MH, Laib A, Thomas T, Ruegsegger P, Alexandre C, Vico L. Tail suspension induces bone loss in skeletally mature mice in the C57BL/6J strain but not in the C3H/HeJ strain. J Bone Miner Res. 2003; 18(3):561–569. [PubMed: 12619942]
51. Knott L, Bailey AJ. Collagen cross-links in mineralizing tissues: a review of their chemistry, function, and clinical relevance. Bone. 1998; 22(3):181–187. [PubMed: 9514209]
52. Wassen MH, Lammens J, Tekoppele JM, Sakkers RJ, Liu Z, Verbout AJ, Bank RA. Collagen structure regulates fibril mineralization in osteogenesis as revealed by cross-link patterns in calcifying callus. Journal of bone and mineral research : the official journal of the American Society for Bone and Mineral Research. 2000; 15(9):1776–1785.
53. Manjubala I, Liu Y, Epari DR, Roschger P, Schell H, Fratzl P, Duda GN. Spatial and temporal variations of mechanical properties and mineral content of the external callus during bone healing. Bone. 2009; 45(2):185–192. [PubMed: 19414072]
54. Burket J, Gourion-Arsiquaud S, Havill LM, Baker SP, Boskey AL, van der Meulen MC. Microstructure and nanomechanical properties in osteons relate to tissue and animal age. J Biomech. 2011; 44(2):277–284. [PubMed: 21074774]
55. Tarnowski CP, Ignelzi MA Jr, Morris MD. Mineralization of developing mouse calvaria as revealed by Raman microspectroscopy. J Bone Miner Res. 2002; 17(6):1118–1126. [PubMed: 12054168]
56. Donnelly E, Boskey AL, Baker SP, van der Meulen MC. Effects of tissue age on bone tissue material composition and nanomechanical properties in the rat cortex. J Biomed Mater Res A. 2010; 92(3):1048–1056. [PubMed: 19301272]
57. Spevak L, Flach CR, Hunter T, Mendelsohn R, Boskey A. Fourier transform infrared spectroscopic imaging parameters describing acid phosphate substitution in biologic hydroxyapatite. Calcif Tissue Int. 2013; 92(5):418–428. [PubMed: 23380987]
58. Raghavan M, Sahar ND, Kohn DH, Morris MD. Age-specific profiles of tissue-level composition and mechanical properties in murine cortical bone. Bone. 2012; 50(4):942–953. [PubMed: 22285889]
59. Busa B, Miller LM, Rubin CT, Qin YX, Judex S. Rapid establishment of chemical and mechanical properties during lamellar bone formation. Calcif Tissue Int. 2005; 77(6):386–394. [PubMed: 16362460]

60. Kobrina Y, Turunen MJ, Saarakkala S, Jurvelin JS, Hauta-Kasari M, Isaksson H. Cluster analysis of infrared spectra of rabbit cortical bone samples during maturation and growth. Analyst. 2010; 135(12):3147–3155. [PubMed: 21038039]

61. Miller LM, Little W, Schirmer A, Sheik F, Busa B, Judex S. Accretion of bone quantity and quality in the developing mouse skeleton. J Bone Miner Res. 2007; 22(7):1037–1045. [PubMed: 17402847]

62. Grabner B, Landis WJ, Roschger P, Rinnerthaler S, Peterlik H, Klaushofer K, Fratzl P. Age- and genotype-dependence of bone material properties in the osteogenesis imperfecta murine model (oim). Bone. 2001; 29(5):453–457. [PubMed: 11704498]

63. Chatterji S, Wall JC, Jeffery JW. Age-related changes in the orientation and particle size of the mineral phase in human femoral cortical bone. Calcif Tissue Int. 1981; 33(6):567–574. [PubMed: 6799168]

64. Roschger P, Grabner BM, Rinnerthaler S, Tesch W, Kneissel M, Berzlanovich A, Klaushofer K, Fratzl P. Structural development of the mineralized tissue in the human L4 vertebral body. J Struct Biol. 2001; 136(2):126–136. [PubMed: 11886214]

65. Paschalis EP, DiCarlo E, Betts F, Sherman P, Mendelsohn R, Boskey AL. FTIR microspectroscopic analysis of human osteonal bone. Calcif Tissue Int. 1996; 59(6):480–487. [PubMed: 8939775]

66. Gourion-Arsiquaud S, Burket JC, Havill LM, DiCarlo E, Doty SB, Mendelsohn R, van der Meulen MC, Boskey AL. Spatial variation in osteonal bone properties relative to tissue and animal age. J Bone Miner Res. 2009; 24(7):1271–1281. [PubMed: 19210217]

67. Miller LM, Vairavamurthy V, Chance MR, Mendelsohn R, Paschalis EP, Betts F, Boskey AL. In situ analysis of mineral content and crystallinity in bone using infrared microspectroscopy of the nu(4) PO(4)(3−) vibration. Biochim Biophys Acta. 2001; 1527(1–2):11–19. [PubMed: 11420138]

68. Roberts JE, Bonar LC, Griffin RG, Glimcher MJ. Characterization of very young mineral phases of bone by solid state 31phosphorus magic angle sample spinning nuclear magnetic resonance and X-ray diffraction. Calcif Tissue Int. 1992; 50(1):42–48. [PubMed: 1739869]

69. Akkus O, Adar F, Schaffler MB. Age-related changes in physicochemical properties of mineral crystals are related to impaired mechanical function of cortical bone. Bone. 2004; 34(3):443–453. [PubMed: 15003792]

70. Turunen MJ, Prantner V, Jurvelin JS, Kroger H, Isaksson H. Composition and microarchitecture of human trabecular bone change with age and differ between anatomical locations. Bone. 2013; 54(1):118–125. [PubMed: 23388419]

71. Granke M, Gourrier A, Rupin F, Raum K, Peyrin F, Burghammer M, Saied A, Laugier P. Microfibril orientation dominates the microelastic properties of human bone tissue at the lamellar length scale. PLoS One. 2013; 8(3):e58043. [PubMed: 23472132]

72. Li C, Paris O, Siegel S, Roschger P, Paschalis EP, Klaushofer K, Fratzl P. Strontium is incorporated into mineral crystals only in newly formed bone during strontium ranelate treatment. J Bone Miner Res. 2010; 25(5):968–975. [PubMed: 19874195]

73. Bunger MH, Oxlund H, Hansen TK, Sorensen S, Bibby BM, Thomsen JS, Langdahl BL, Besenbacher F, Pedersen JS, Birkedal H. Strontium and bone nanostructure in normal and ovariectomized rats investigated by scanning small-angle X-ray scattering. Calcif Tissue Int. 2010; 86(4):294–306. [PubMed: 20221590]

74. Zizak I, Roschger P, Paris O, Misof BM, Berzlanovich A, Bernstorff S, Amenitsch H, Klaushofer K, Fratzl P. Characteristics of mineral particles in the human bone/cartilage interface. J Struct Biol. 2003; 141(3):208–217. [PubMed: 12648567]

Highlights

- Loading led to enhanced collagen maturity in elderly mice.
- Bone formed in response to controlled or physiological loading had similar quality.
- Mineral and matrix properties were tissue age and animal age dependent.
- Material quality of new bone differed between endosteal and periosteal regions.

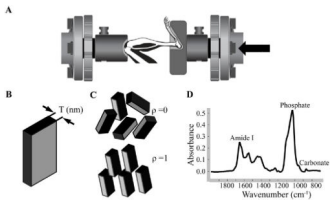

Fig.1.

(a) Mouse tibia within loading device (arrow indicates force direction); (b) T parameter corresponds to mean mineral thickness; (c) ρ parameter varies between 0 (randomly oriented mineral particles) and 1 (perfectly aligned mineral particles); (d) Cortical bone FTIRI spectrum

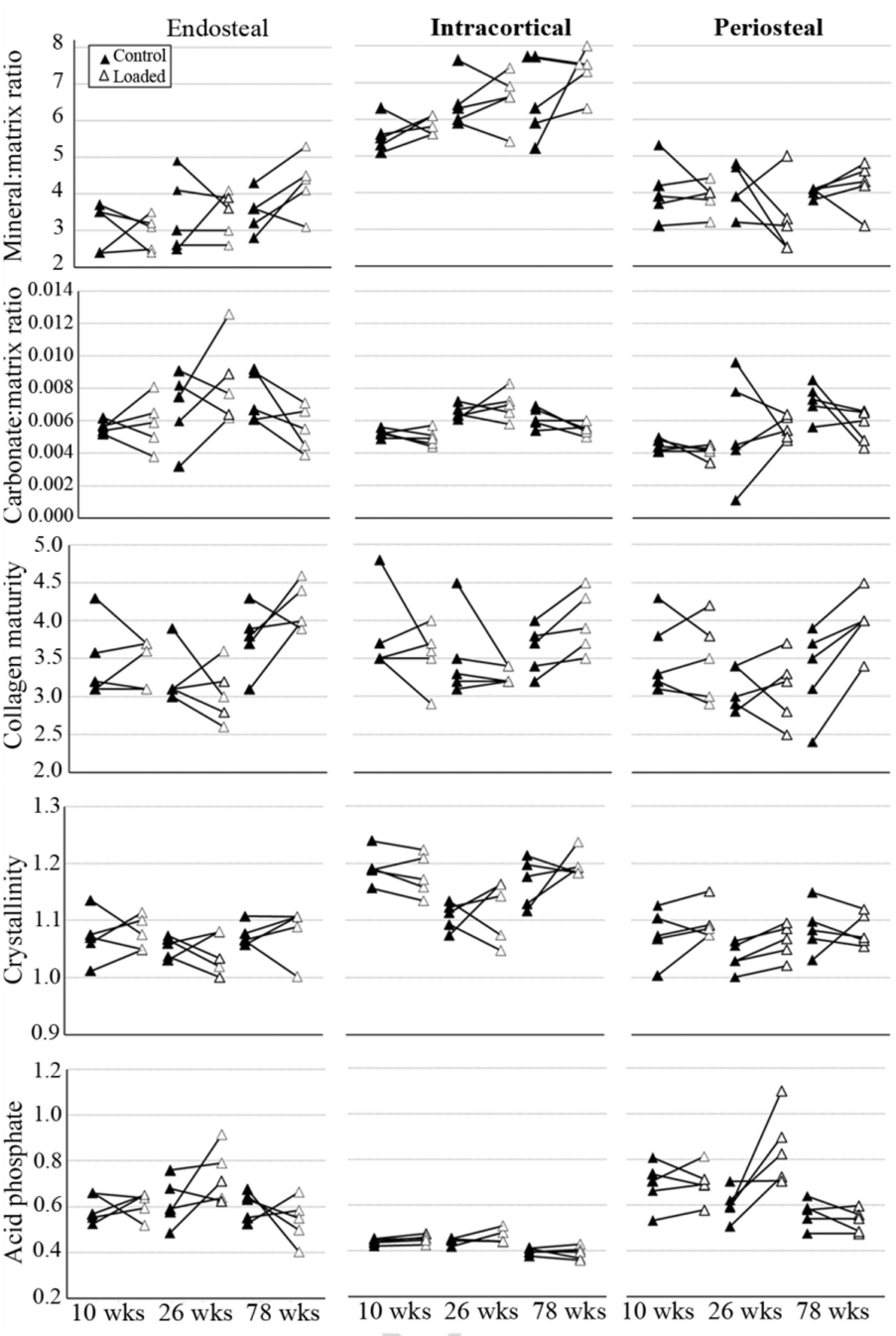

Fig.2.

Regional (endosteal, intracortical, periosteal) changes in FTIRI parameters between right (control)-left (*in vivo* loaded) paired tibiae from individual mice as a function of age. The differences measured between loaded and control limbs are generally smaller than regional differences for each mouse

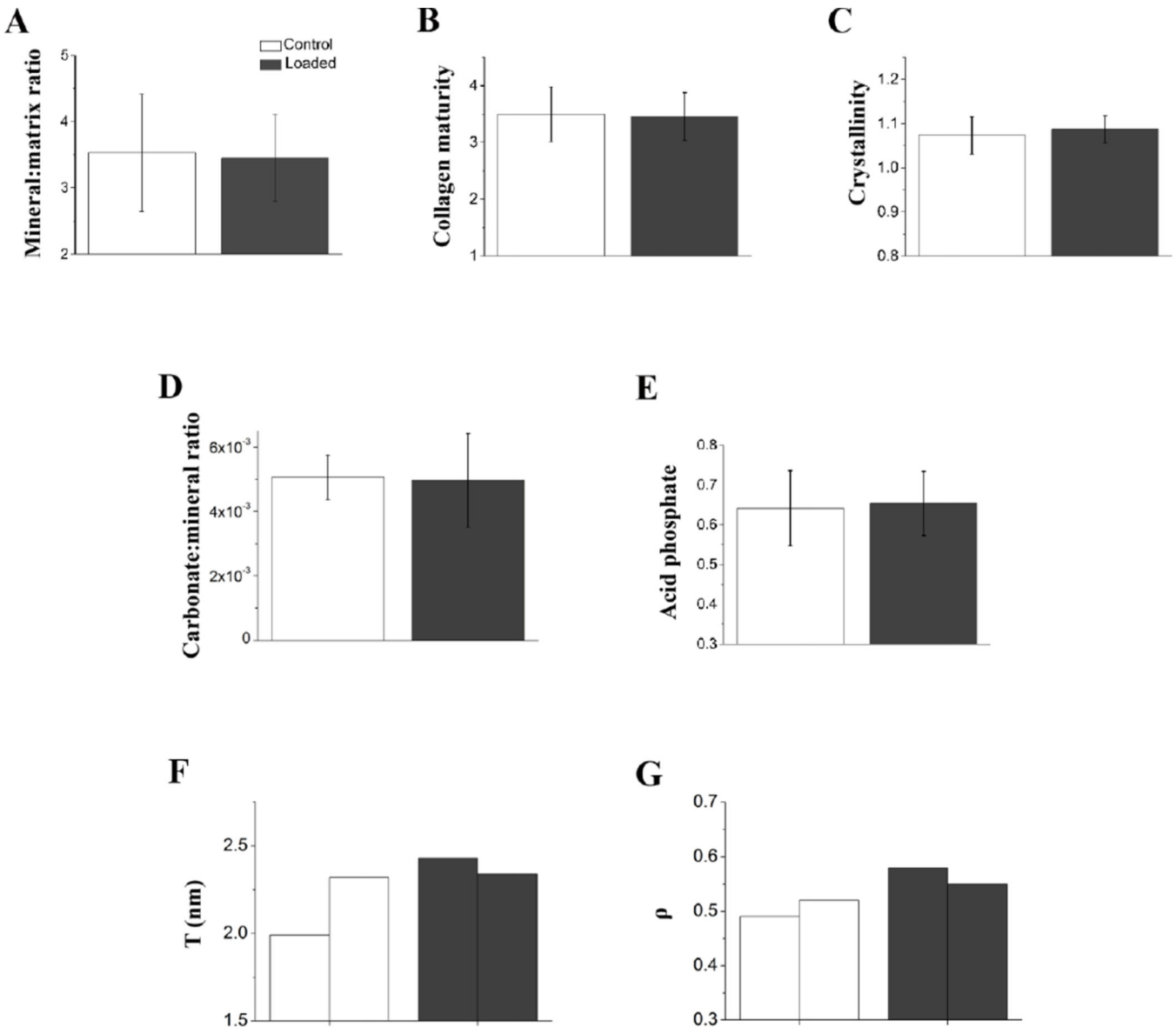

Fig.3.

Newly formed tissue within the endosteal and periosteal regions were pooled and compared between the *in vivo* loaded and control limbs of 10 week old mice. These data show that that the newly formed tissue with *in vivo* loading had similar material quality to new tissue formed during physiological loading. (a) Mineral:matrix ratio; (b) collagen maturity; (c) crystallinity; (d) carbonate:mineral ratio; (e) acid phosphate; The mean comprises pooled tissue at the endosteal and periosteal regions and bars represent standard deviations (n=5 in (a–e)). (f) T parameter and (g) ρ parameter of the individual values obtained at the endosteal and periosteal regions of the control and loaded limbs of 10 week old mice (each bar corresponds to one tibia)

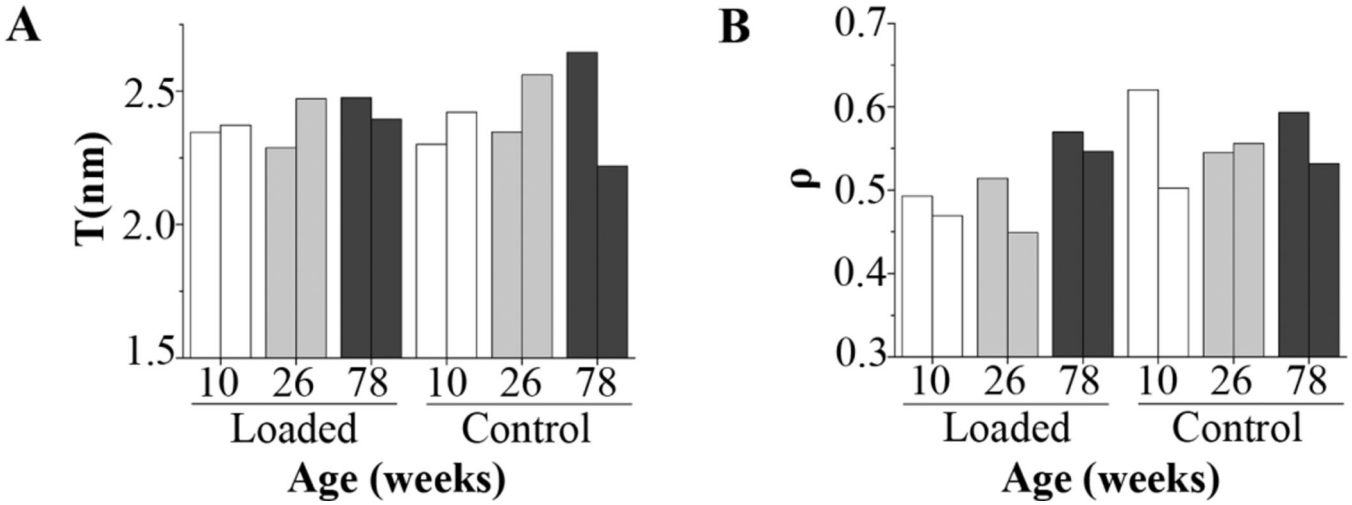

Fig.4.

(a) T and (b) ρ parameters at the intracortical region of control and loaded tibiae from n=2 mice/age (each bar corresponds to one tibia)

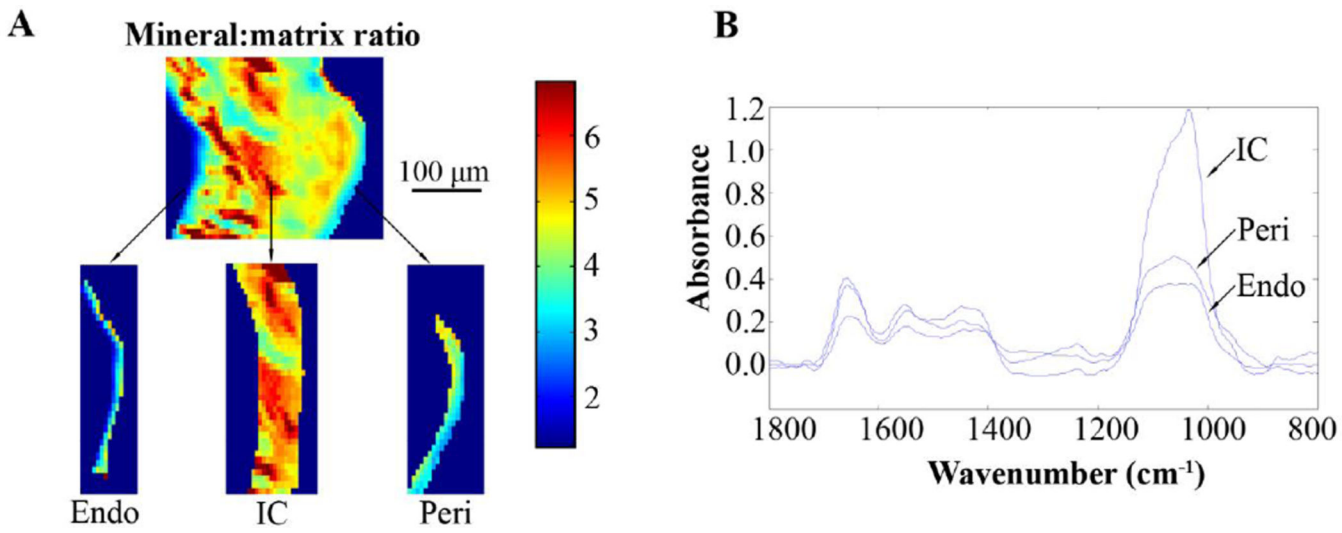

Fig.5.

Regional differences reflecting tissue age were observed in the measured parameters. (a) Mineral:matrix ratio higher in the intracortical (IC) region than in the endosteal (Endo) or periosteal (Peri) regions of the control tibia of a 26 week old mouse; respective (b) FTIRI spectra

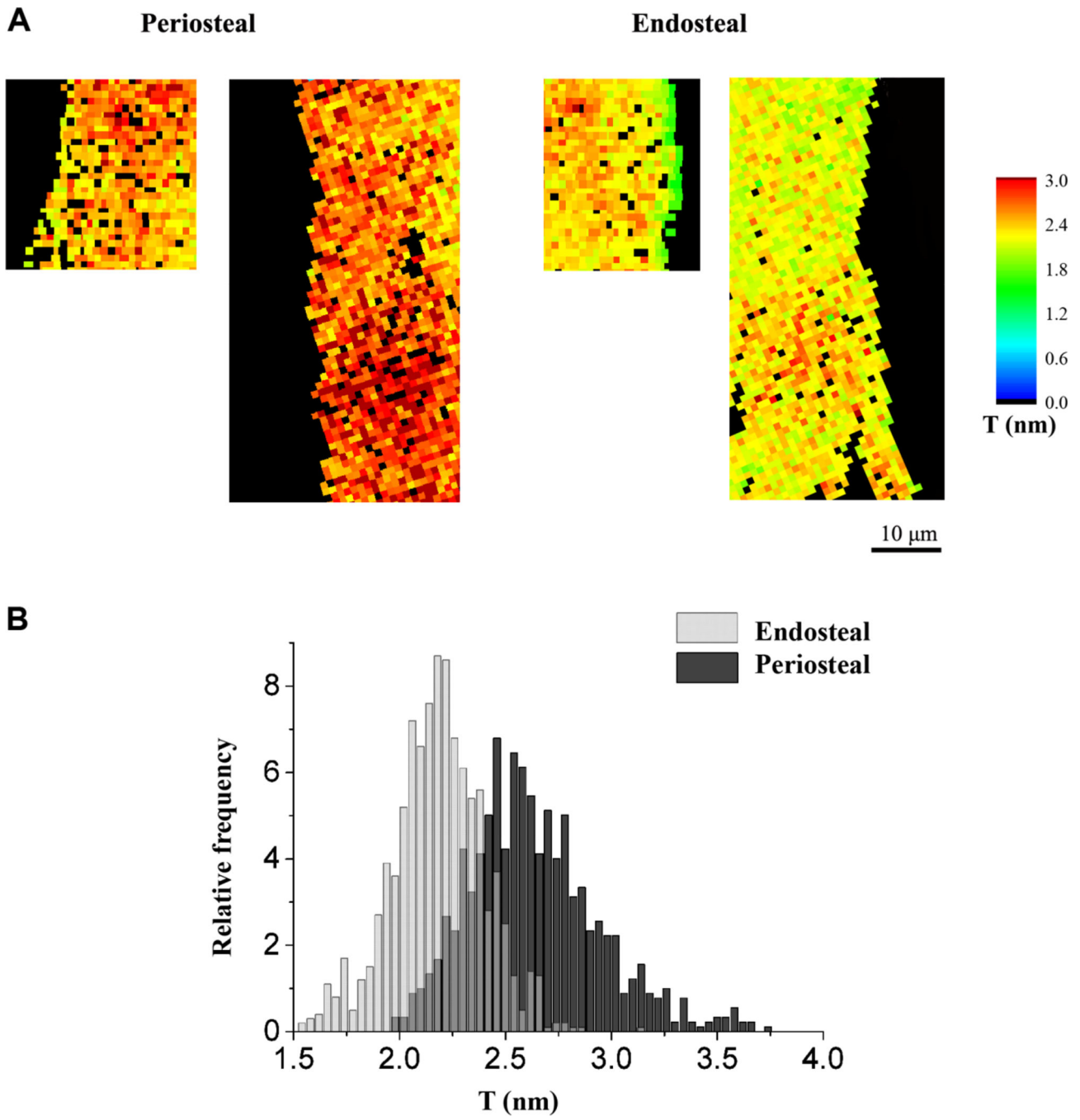

Fig.6.

Regional differences showing lower mean mineral thickness in the endosteal compared to periosteal new tissue formed in response to loading: (a) maps and (b) histogram of the T parameter (binning=0.02) of all the measured points at the endosteal and periosteal regions of the loaded limbs of two 10 week old mice

Table 1

Mean values and standard deviations (n=5) of parameters analyzed with FTIRI at the endosteal, intracortical and periosteal regions for 10, 26 and 78 week old mice.

	10 wk		26 wk		78 wk	
	Loaded	**Control**	**Loaded**	**Control**	**Loaded**	**Control**
Mineral:Matrix[a,b]						
Endosteal	2.94 ±0.47[f,g]	3.10 ±0.64[g]	3.44 ±0.63[g]	3.52 ±0.97[g]	4.36±0.65[d,e,g]	3.50 ±0.56[g]
Intracortical	5.84 ±0.25	5.64 ±0.62	6.58 ±0.74	6.44 ±0.68	7.32 ±0.63	6.56 ±1.11
Periosteal	3.96 ±0.30[g]	3.96 ±0.94[g]	3.30 ±1.02[g]	4.08 ±0.69[g]	4.20 ±0.66[g]	4.02 ±0.13[g]
Crystallinity[a,b]						
Endosteal	1.08 ±0.03[g]	1.07 ±0.04[g]	1.04 ±0.39[g]	1.05 ±0.02[g]	1.08 ±0.04[g]	1.08 ±0.02[g]
Intracortical	1.18 ±0.04	1.19 ±0.03[e]	1.12 ±0.05	1.11 ±0.02	1.20 ±0.02[e]	1.17 ±0.04[e]
Periosteal	1.10 ±0.03[g]	1.08 ±0.05[g]	1.06±0.03[d]	1.04 ±0.03[g]	1.08 ±0.03[g]	1.09 ±0.04
Collagen maturity[a,b,c]						
Endosteal	3.4 ±0.3	3.4 ±0.3[g]	3.0 ±0.4	3.2 ±0.4	4.2 ±0.3[e]	3.8 ±0.4[f]
Intracortical	3.5 ±0.4	3.8 ±0.6	3.3 ±0.1	3.5 ±0.6	4.0±0.4[d,e]	3.6 ±0.3
Periosteal	3.5 ±0.5	3.5 ±0.5	3.1 ±0.5	3.1 ±0.3	4.0 ±0.4[d,e]	3.3 ±0.6
Carbonate:Mineral × 1000[a,b]						
Endosteal	5.9 ±1.6[f]	5.6 ±0.4[f]	8.4 ±2.6	6.8 ±2.3	5.5 ±1.3	7.4 ±1.6
Intracortical	4.9 ±0.5[e]	5.2 ±0.3[e]	7.0 ±0.9	6.5 ±0.4	5.5 ±0.4[e]	6.2 ±0.6
Periosteal	4.1 ±0.4[g]	4.5 ±0.4[g,e]	5.6 ±0.7[g]	5.4 ±3.3	5.6 ±1.0	7.2 ±1.1[g]
Acid Phosphate[a,b,c]						
Endosteal	0.61 ±0.06[g]	0.59 ±0.06[g]	0.74 ±0.12[g]	0.62 ±0.11[g]	0.54±0.04[g,e]	0.60 ±0.06[g]
Intracortical	0.45 ±0.02[d]	0.44 ±0.01	0.46 ±0.03	0.45 ±0.01	0.39 ±0.03[e]	0.40 ±0.01[e]
Periosteal	0.70 ±0.08[g]	0.69 ±0.10[g]	0.85±0.16[f,g]	0.60 ±0.07[g]	0.53±0.05[g,e]	0.60 ±0.08[g]

[a]Between-subject effects of animal age,

[b] Within-subject effects of region,

[c] Interactions between animal age and loading, ANOVA, p<0.05

[d] Different from control, paired t-test p<0.05

[e] Different from 26 week old, unpaired t-test p<0.05

[f] Different from Periosteal,

[g] Different from Intracortical; paired t-test p<0.05

Table 2

Mean values and standard deviations (n=5) of endocortical and periosteal bone formation indices parameters for 10, 26 and 78 week old mice. The 10 and 26 week old mice were a subset from a larger group, which was previously reported [17].

	10 wk		26 wk		78 wk	
	Loaded	**Control**	**Loaded**	**Control**	**Loaded**	**Control**
Ec.sLS/BS (%)[a]	12.1±2.9	14.8±9.4	23.7±19.4 (n=4)	24.4±10.5	28.6±9.3	30.4±4.9
Ec.dLS/BS (%)[a]	85.4±5.5	79.0±11.6	34.7±20.0 (n=4)	19.5±9.5	14.3±4.0	12.2±10.3 (n=4)
Ec.MS/BS (%)[a,b]	91.5±4.8	86.4±10.2	46.6±11.1 (n=4)	31.7±9.2	28.5±6.4	25.0±9.8
Ec.MAR (μm/day)[b,c]	2.02±0.23[d]	0.94±0.25	1.81±0.33 (n=4)	0.91±0.35	1.29±0.38	1.51±0.63 (n=4)
Ec.BFR/BS (μm/day)[a, b,c]	1.85±0.22[d]	0.83±0.29	0.84±0.24 (n=4)	0.29±0.16	0.39±0.21	0.40±0.15 (n=4)
Ps.sLS/BS (%)	23.9±10.8[d]	44.1±30.4	16.0±8.6 (n=4)	26.5±28.1	32.1±19.0	37.4±9.2
Ps.dLS/BS (%)[b]	59.3±15.5[d]	12.6±13.7	42.4±26.2 (n=4)	14.3±10.3 (n=4)	4.7±1.1 (n=2)	2.4 (n=1)
Ps.MS/BS (%)[a,b,c]	71.2±12.0[d]	34.7±8.1	50.4±28.9 (n=4)	27.6±21.8	17.9±10.5	19.2±4.0
Ps.MAR (μm/day)[b,c]	1.83±0.48[d]	0.51±0.14	1.16±0.37 (n=4)	0.74±0.10 (n=4)	1.22±0.67 (n=2)	1.39 (n=1)
Ps.BFR/BS (μm/day)[b]	1.32±0.47[d]	0.18±0.06	0.64±0.52 (n=4)	0.21±0.17 (n=4)	0.32±0.20 (n=2)	0.22 (n=1)

[a] Between-subject effects of animal age,

[b] Within-subject effects of loading,

[c] Interactions between animal age and loading, ANOVA, $p<0.05$

[d] Different from control, paired t-test $p<0.05$

Note: Although 5 mice per age were studied, some mice did not have single or double calcein labels present; in this case the number of mice with labels is indicated in the table.